

TD - 03 - 029  
June 16, 2003

## HFDM-02 Mirror Magnet Production Report

**D. R. Chichili<sup>1</sup>, G. Ambrosio<sup>2</sup>, N. Andreev<sup>1</sup>, E. Barzi<sup>2</sup>,  
V. Kashikhin<sup>1</sup>, V. Kashikhin<sup>2</sup>, S. Yadav<sup>1</sup>,  
R. Yamada<sup>2</sup>, and A. Zlobin<sup>2</sup>**

*<sup>1</sup>Engineering and Fabrication Department*

*<sup>2</sup>Development and Test Department*

*Technical Division*

*Fermilab, Batavia, IL 60510*

## 1.0 INTRODUCTION

HFDM-02 was the first mirror magnet to be tested with a new half-coil. Several changes were made in HFDM-02 to improve the quench performance and are listed below –

- ❑ Bare cable was annealed in argon atmosphere to avoid oxidation of copper. Note that for all the previous magnets, cable was annealed in air.
- ❑ The cable was insulated for the first time with pre-peg ceramic insulation tape. Liquid binder was not added at any stage of cable insulation or coil winding or curing.
- ❑ Each end-saddle had holes underneath the splice joints to improve cooling.
- ❑ The azimuthal size of the cured half-coil was at the nominal so that the heat-treatment occurs under pressure similar to other shell-type and racetrack coils made elsewhere. Note that all previous coils with the exception of HFDA-01 coils were reacted with 1.0 mm gap between the top plate of the reaction fixture and the mid-plane of the coil.
- ❑ The coil was reacted without the inner mandrel to allow for cable expansion inside the bore. This will reduce possible cable stress/strain and also improve conditions for gas removal from the coil before and during reaction.
- ❑ Reaction and impregnation tooling were inspected and modified to reduce the bow shape observed in all previous coils [TD-03-025].
- ❑ Two NbTi lead cables (one on either side of Nb<sub>3</sub>Sn cable) were used for splice joints. In the previous magnets a combination of NbTi and Cu lead cables were used from one side.
- ❑ Horizontal split yoke design was implemented to ease the assembly process and to be able to change the pre-stress in the coil through the addition of mid-plane shim.
- ❑ The amount of pre-stress in the coil was kept under 75 MPa to eliminate any possible degradation of the conductor.
- ❑ The entire magnet was assembled with stainless steel yoke to gain pre-stress during cool down. Furthermore, it would give a uniform loading along the length of the coil.

## 2.0 STRAND & CABLE

The strand was made by Oxford using Modified Jelly Roll process. The strand diameter is 1.0 mm with a filament diameter of approximately 110  $\mu\text{m}$ . Rutherford type cable with 28 strands was manufactured at Fermilab. Table 1 lists the cable parameters. Note that the cable has 25  $\mu\text{m}$  thick and 9.5 mm wide annealed 316L stainless steel core between the two layers.

The cable was heat-treated at 200 °C for 30 min in argon atmosphere to reduce the residual twist in the cable that comes from the cabling process. Four virgin and four extracted strand samples were

placed as witness samples in the reaction fixture along with the coil assembly. The samples were placed along the length of the retort to check if there is any variation in temperature that would result in  $I_c$  degradation. Fig. A1 shows the placement of these witness samples inside the retort. Appendix at the end of the report describes the measurements made at the short sample test facility. Based on these measurements the short sample limit of the magnet is about 25230 A for a  $B_0$  of about 8.4 T and a  $B_{max}$  of about 11.3 T.

PARAMETER	UNIT	VALUE
Mid-Thickness	mm	1.7994
Width	mm	14.242
Keystone angle	deg	0.918
Pitch Length	mm	109.8
Number of Strands		28
Lay Direction		Left
Reel Number		HFDA-020513-28-2

**Table 1:** *Cable parameters.*

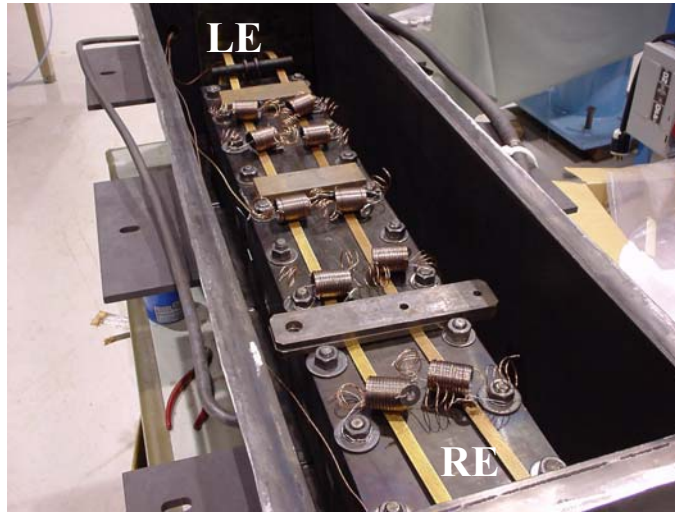


**Fig. A1:** *Witness samples inside the retort.*

### 3.0 COIL FABRICATION

#### 3.1 Pre-peg Ceramic Insulation

After a series of discussions between Fermilab and Composite Technology Development Inc., the company produced their first version of the pre-peg ceramic tape. To benchmark the thickness of the tape, the height of the ten-stack samples insulated with different percentage overlaps of pre-peg tape were measured and compared with that of the previous magnets. Fig. 1 shows the test data.

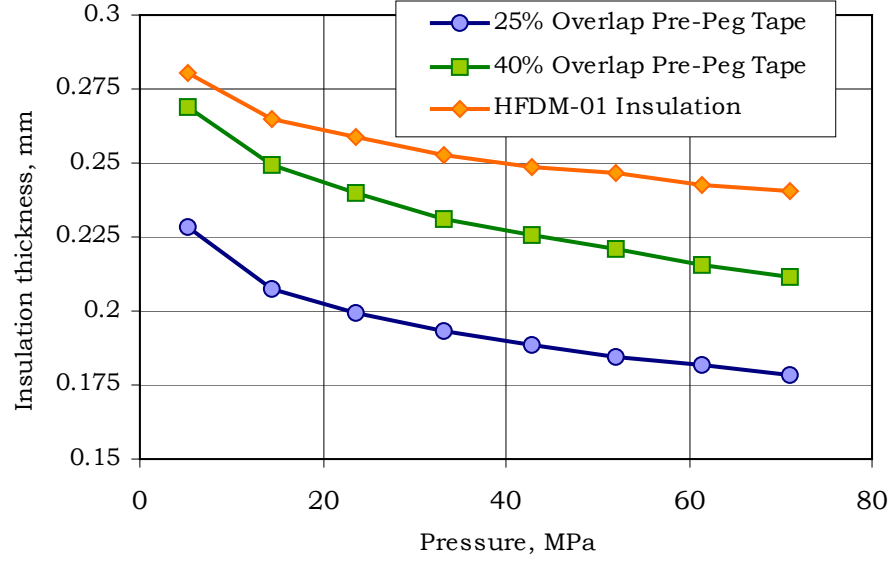


**Fig. 1:** *Variation of the insulation thickness with % overlap and pressure.*

### 3.2 Coil Winding and Curing

Based on the insulation thickness measurements, the cable was insulated with 45% overlap pre-peg ceramic tape. Winding and curing procedures were similar to that of the previous magnets. Liquid binder was applied to the wedges to improve adhesion to the cable turns. The curing pressure was about 25 MPa and the curing temperature ranged from 150 to 160 °C for 30 mins. Fig. 2 shows the half-coil after curing.

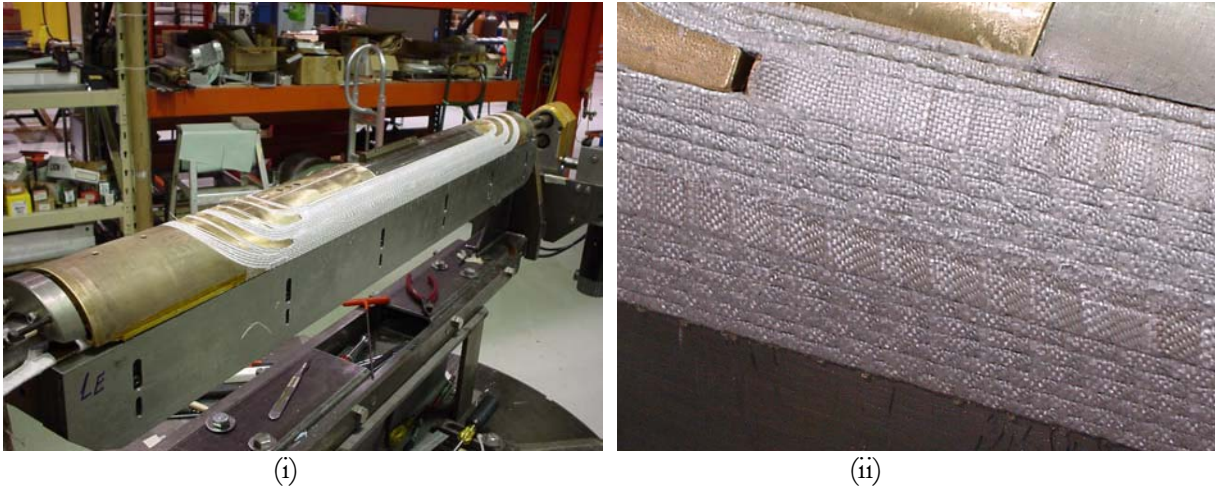


**Fig. 2:** *(i) Cured half coil. (ii) Higher magnification picture of the coil. The insulation was quite strong and the quality of the cured coil was one of the best we have made thus far.*

### 3.3 Coil Measurements

The azimuthal size of the coil was measured to determine if the coil needed to be shimmed during reaction. Note that we wanted the coil to be at the nominal size after curing so that the heat-treatment process would take place under pressure. Fig. 3 shows the data. The measurements were stopped at a pressure of 10 MPa to minimize local deformation.

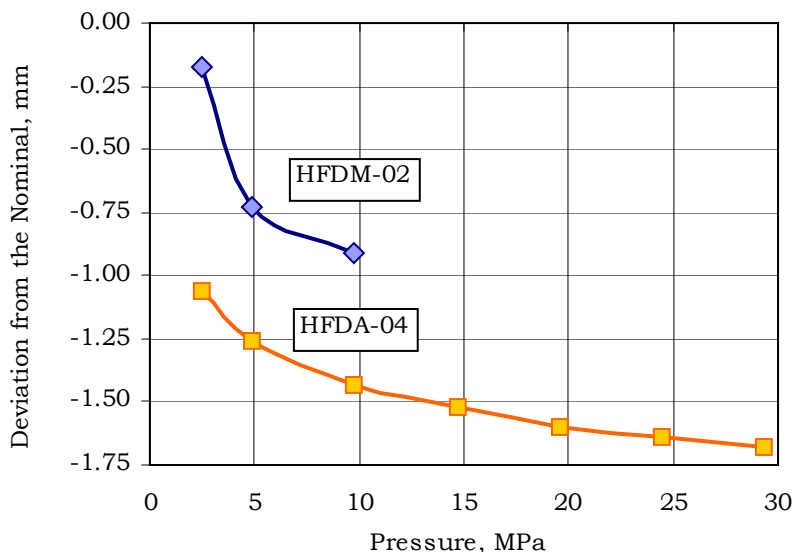


**Fig. 3:** *Azimuthal coil size measurements. HFDA-04 data was included for comparison.*

Electrical measurements were taken before placing the coil into the reaction fixture to check for possible turn-to-turn shorts. The data is shown in Table 3. The values are similar to that of previous half-coils fabricated, which indicate that the coil is free from turn-to-turn shorts. Note that L and Q were measured at 1 kHz and the resistance was measured using four-wire technique at 0.1 A.

	RESISTANCE, m $\Omega$	INDUCTANCE, $\mu$ H	Q
HFDAH-10	55.59	220.4	5.67

**Table 3:** *Half-coil electrical measurements*

### 4.0 COIL REACTION

The mid-plane lead turn for both inner and outer layer were first separated after curing to avoid risk of cable damage during splicing. The half-coil was then shimmed up to the nominal size. Two pieces of ceramic cloth each 0.125 mm thick was placed as shims in the mid-plane as shown in Fig. 4. The coil was then placed in one half of the reaction fixture and secured using the top plate. The second half of the reaction fixture was also used as a dummy to reduce the bow in the fixture assembly. The reaction cycle followed was similar to that of previous magnets (see Table 4). Thermocouples were attached to the either end of the coil to measure the temperature profile. Coil was carefully removed from the reaction fixture and placed on wooden blocks (see Fig. 5). The integrity of coil turns after reaction was very good.



**Fig. 4:** *Mid-plane shim on the coil.*

	RAMP RATE, °C/HR	TEMPERATURE, °C	DWELL TIME, HR.
Step - 1	25	210	100
Step - 2	50	340	48
Step - 3	75	650	180

**Table 4:** *Heat-treatment cycle used in HFDM-02.*



**Fig. 5:** *(i) Reacted coil. (ii) Closer view of the outer layer of the coil*

## 5.0 SPLICE JOINTS

Two NbTi lead cables, one on either side of the Nb<sub>3</sub>Sn cable were carefully inserted. The lead cables were pre-tinned for better splice joints. The procedure followed was very similar to that of HFDA-04 [TD-02-025]. The cable motion was carefully monitored during the entire operation using several dial indicators as shown in Fig. 6(i). A maximum vertical motion of about 0.4 mm was recorded on

the inner Nb<sub>3</sub>Sn cable and 0.17 mm was recorded on the outer Nb<sub>3</sub>Sn cable near the splice joints as shown by arrows in Fig. 6(ii) during inner and outer splicing operations respectively.

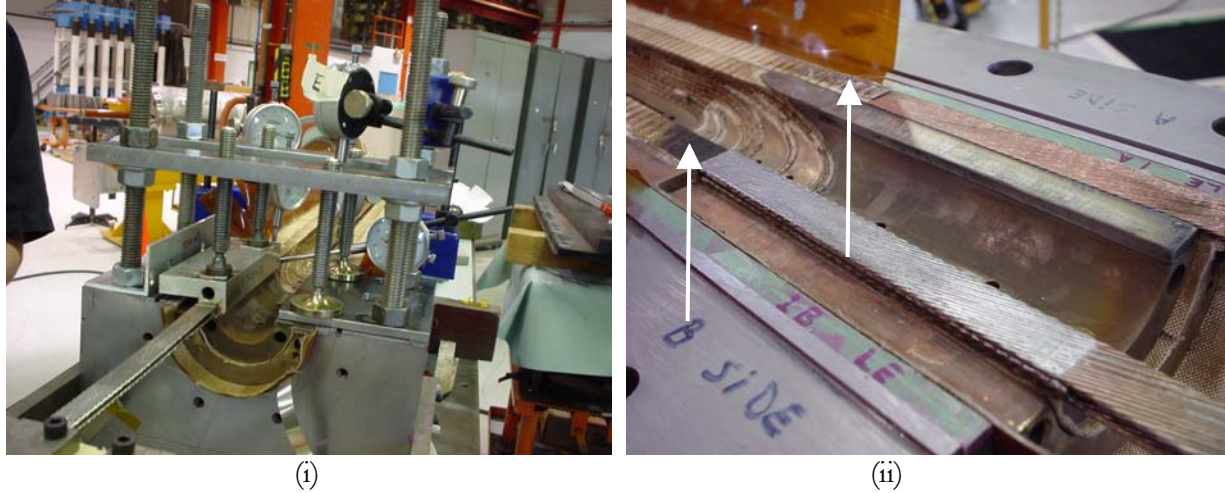


**Fig. 6:** (i) Setup for splice joints. (ii) Finished inner layer splice joint.

## 5.0 EPOXY IMPREGNATION

Before proceeding with the coil impregnation, several studies were conducted on the shape of the coil to check for systematic deviations from nominal. HFDA-04 coils were used in the study. Fig. 7 shows the cylindrical and mid-plane variation along the length of the coil. Both surfaces show a peak-to-peak variation of 0.7 mm. This could be attributed to either tooling shape or process related.

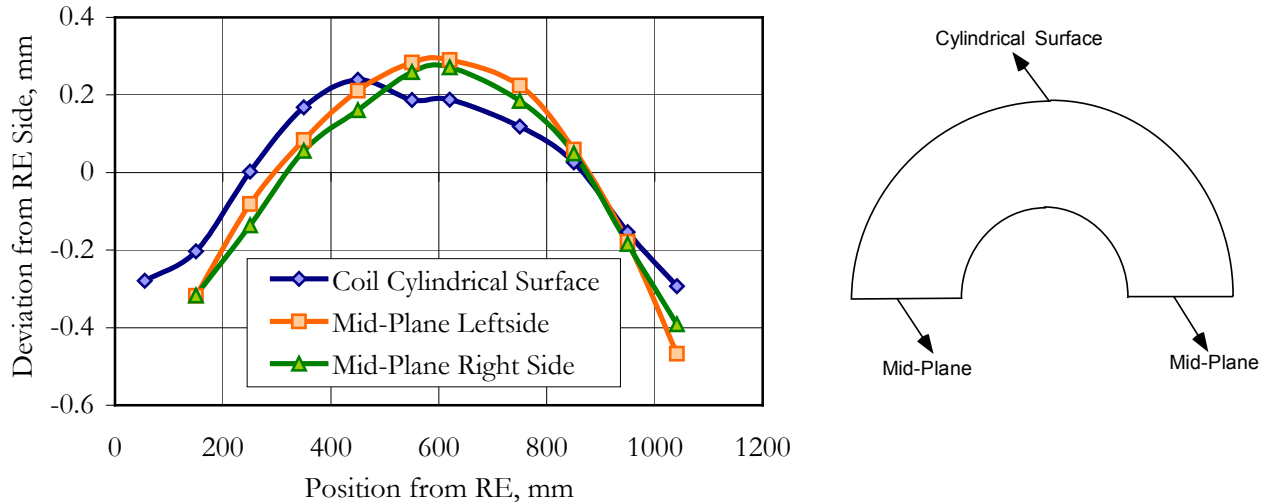


**Fig. 7:** Variation of HFDA-04 coil cylindrical and mid-plane surfaces along the length.

Impregnation tooling was then measured using CMM to correlate with the shape of HFDA-04 coil. Fig. 8 shows the findings along with the original or “as received” data. The tooling shape has degraded over time. The V-shape of the cylindrical surface is due to the machining from each end to center of the fixture and it got worse over time. On the other-hand, the shape of the mid-plane changed from sloping surface to the U-shape.

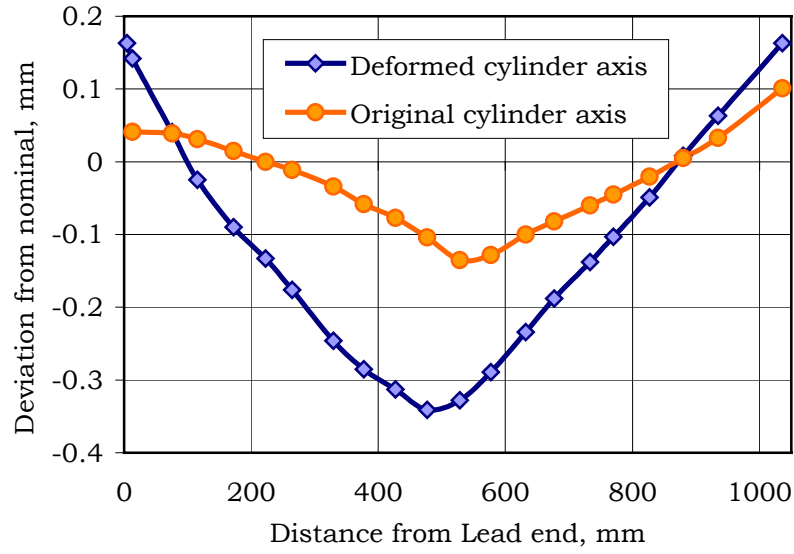


**Fig. 8 (i):** *Variation of the cylindrical surface of the impregnation tooling*

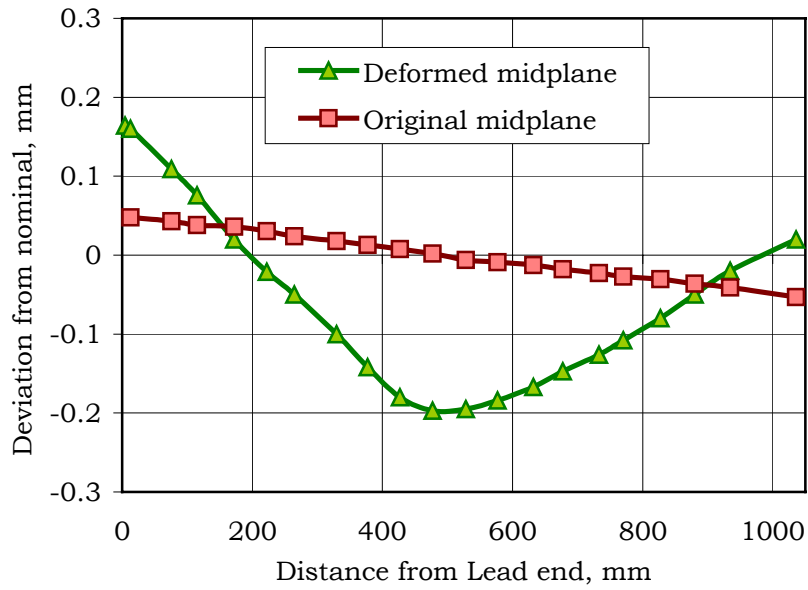


**Fig. 8 (ii):** *Variation of the mid-plane surface of the impregnation tooling*

To reduce the bow in the tooling the two halves were welded under pressure as shown in Fig. 9 and the measurement data for the modified fixture are shown in Fig. 10. More detailed description of these measurements can be found in the tech note, TD-03-025.



**Fig. 9:** *Modified Tooling*

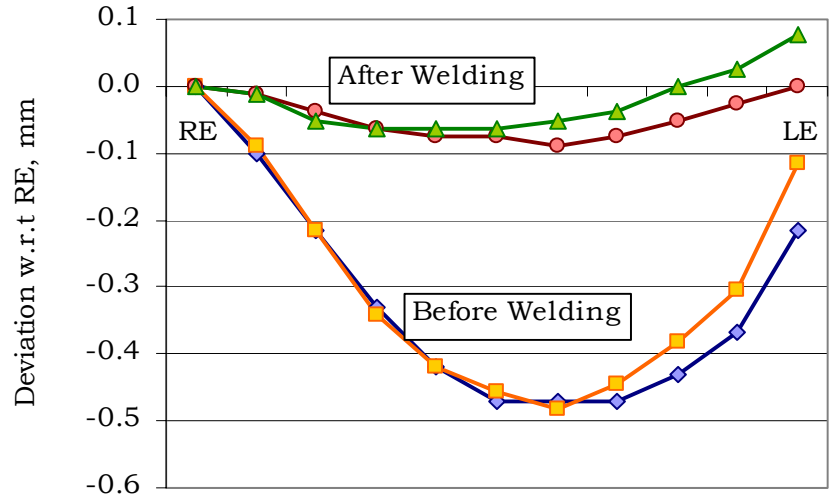


**Fig. 10:** *Variation of the mid-plane after modification*

Finally Fuji film experiments on HFDA-04 coils revealed stress concentration near the mid-plane along the length of the coil (see Fig. 11). This was attributed to the clearance in the shim, which was used to fill the gap in the mid-plane of the impregnation fixture. Custom shim was made out of green-putty using HFDA-03 coils to fill this gap (see Fig. 12(i)).

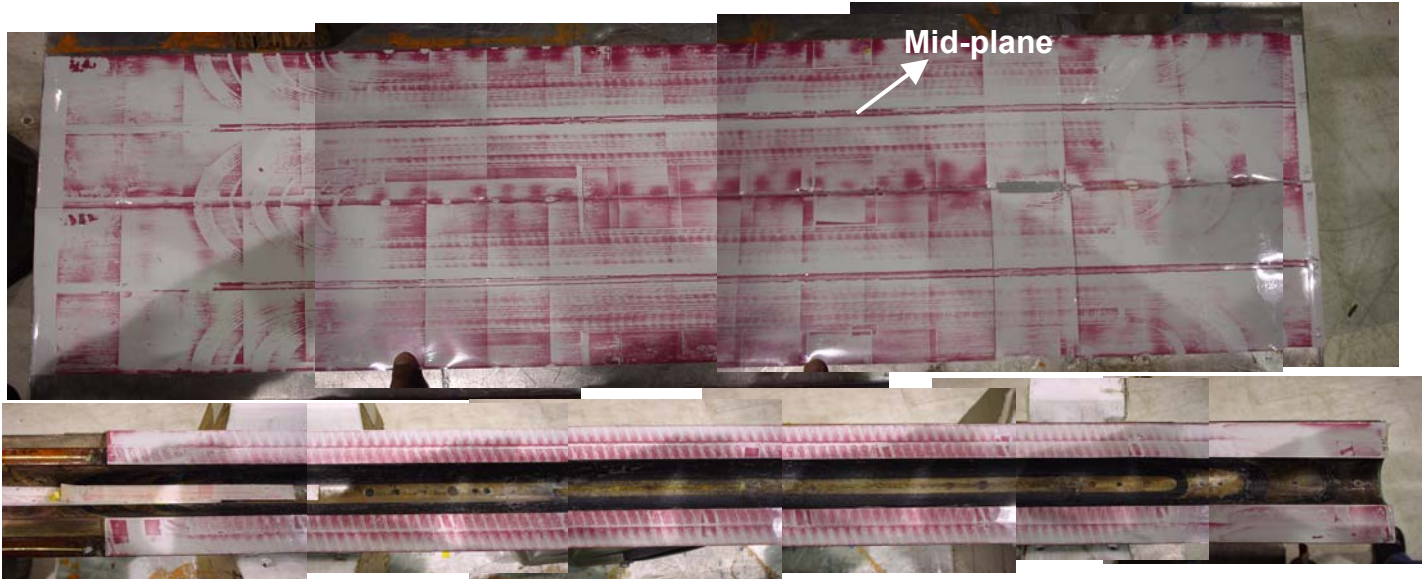


**Fig. 11:** *Fuji film trace of HFDA-04 coils after yoking operation. Top one shows the radial surface and the bottom one the mid-plane. The stress is quite uniform along the length of the coil except at the mid-plane and tapers of at the end.*

With all the aforementioned improvements in the tooling, HFDM-02 coil was assembled for impregnation. The actual procedure was similar to that of the previous magnets. Fig. 12 (ii)

shows the impregnated coil. The shape of the impregnated coil was then measured to see if there were some improvements. Fig. 13 shows the data. The variation in the cylindrical surface was reduced from  $\pm 0.3$  mm to  $\pm 0.1$  mm. The mid-plane however, still has a bow shape leading us to believe that this shape is not related to tooling. Preliminary bench tests indicated that the shape could be a result of differential thermal expansion between the aluminum bronze pole pieces & wedges and coil. More work needs to be done in this direction.



**Fig. 12:** (i) Coil assembled inside the impregnation fixture with new shim (ii) impregnated coil.

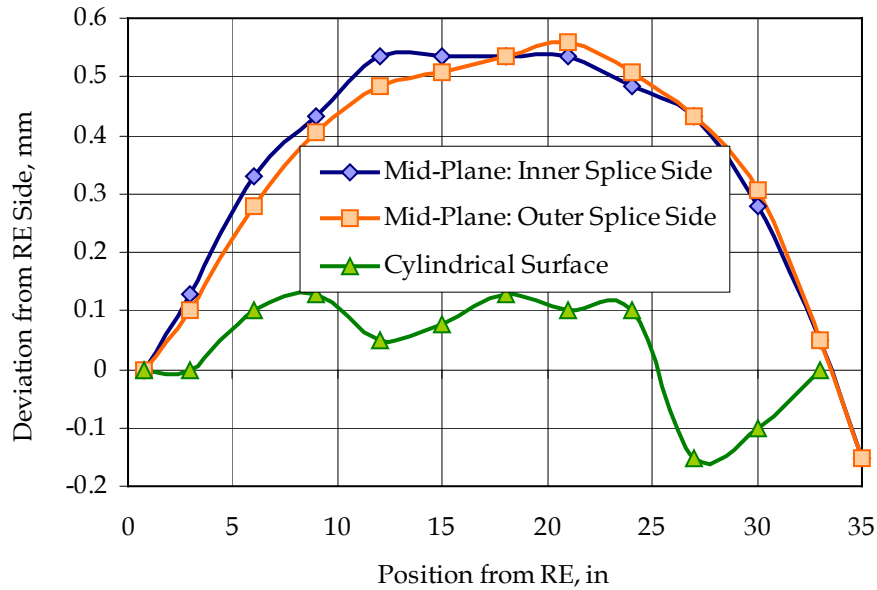


**Fig. 13:** Variation of HFDM-02 coil cylindrical and mid-plane surfaces along the length.

Electrical measurements were performed on the impregnated coil assembly. Table 5 shows the data. For comparison measurements taken before reaction were also included in the table. The resistance of the coil assembly after reaction increased by about 66% due to conversion of copper into bronze

during reaction. The  $Q$  decreased, as the inductance of the coil remained constant before and after reaction. Note that  $L$  and  $Q$  were measured at 1 kHz and the resistance measurements were done at 0.1 A using four wire measuring technique.

	RESISTANCE, $m\Omega$	INDUCTANCE, $\mu H$	$Q$
HFDAH-10 (BEFORE REACTION)	55.59	220.4	5.67
HFDAH-10 (AFTER REACTION)	92.21	205.6	4.04

**Table 5:** *Electrical measurements before and after reaction.*

## 6.0 INSTRUMENTATION

Capacitance gauges were installed both in the outer layer pole region and in the inner layer mid-plane. The gauges were calibrated both at room temperature and at 4.2 K. Two aluminum bronze spacers, one near the LE and one in the straight section were instrumented with resistive strain gauges to measure azimuthal stress. The initial zero readings were taken both at room temperature and at 4.2 K.

Spot heaters were installed in the straight section for temperature studies. Two spot heaters were placed at each location to cover one transposition pitch of the cable. Fig. 15 shows the layout. However, we lost three out of the four heaters during yoking/clamping operation. We are still investigating the reasons for such a high failure rate. The spot heater installation procedure needs to be looked into for future magnets. Several voltage taps were also installed. The schematic layout is shown in Fig. 16.

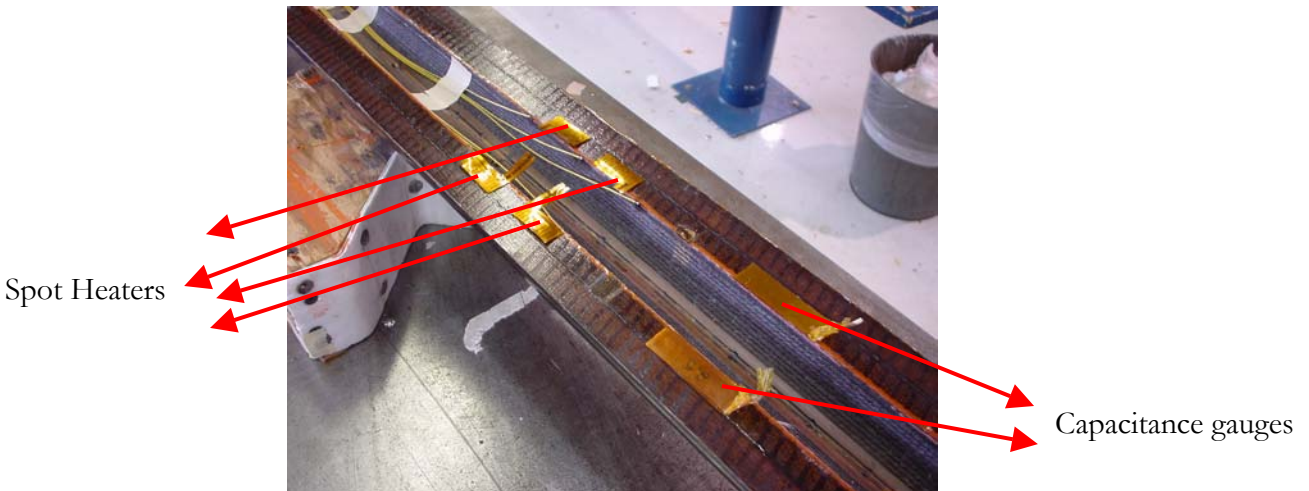


**Fig. 15:** *Photograph showing spot heater and capacitance gauge placements.*

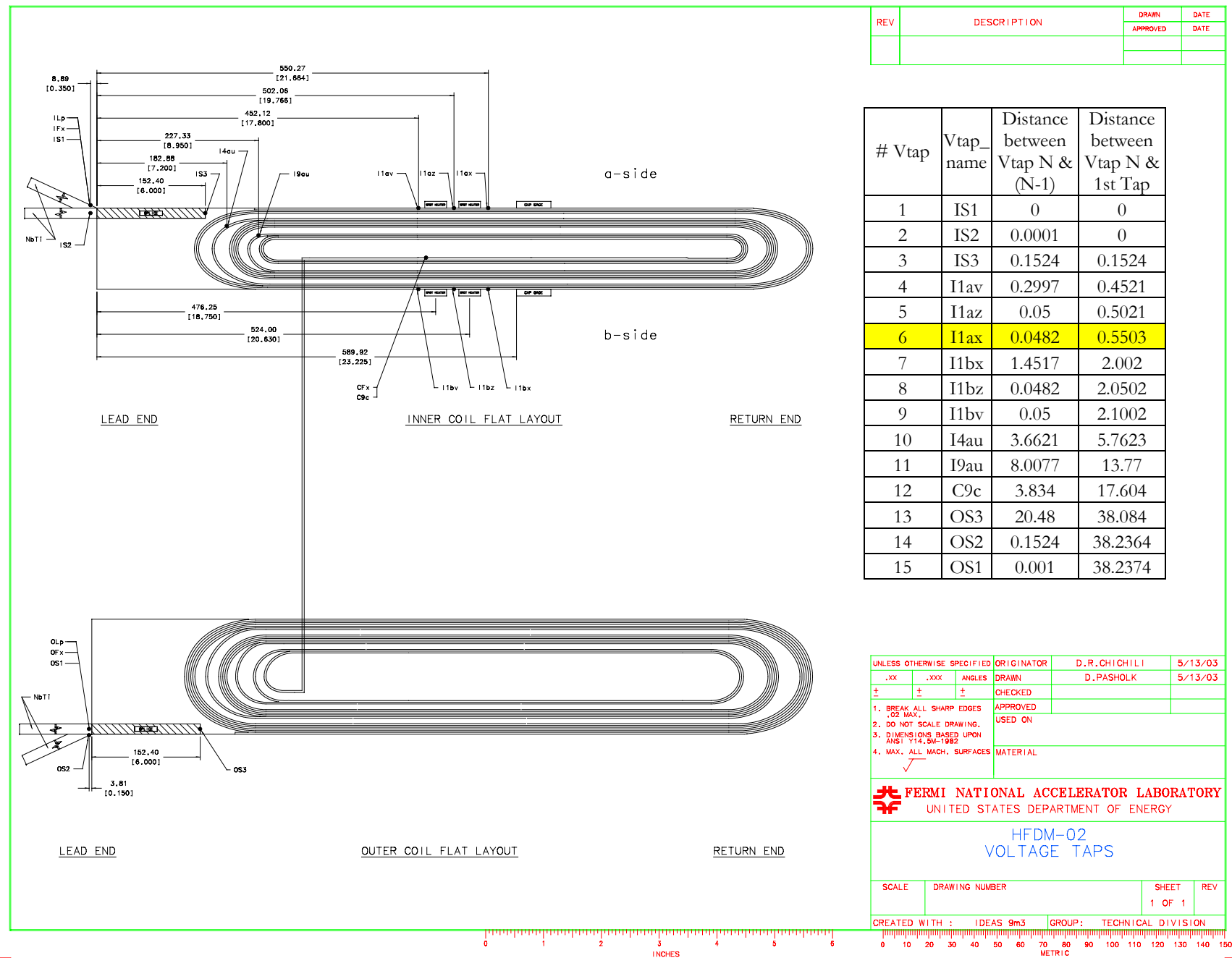
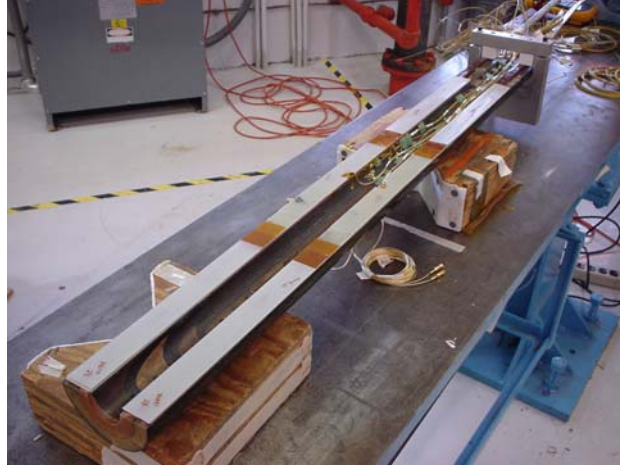


Fig. 16: Voltage tap layout for HFDM-02

## 7.0 MAGNET ASSEMBLY

The mid-plane of the coil assembly was first filled with G10 shims (about 2.5 mm in height). Fig. 17 shows the coil with dry shims placed on top. The shimming was actually graded to account for the shape of the coil.



**Fig. 17:** *Mid-plane shimming of the half-coil. The shims were glued in place inside the yoke assembly.*

The shims were glued in place inside the yoke assembly to obtain the right shape. The procedure followed is as follows – the coil assembly along with spacers was first placed in the lower yoke assembly. Epoxy was applied to each G10 shim and placed on the mid-plane of the coil. Iron mirror was then placed on top of the coil assembly. The upper yoke half was then slowly lowered on top of the iron mirror. The entire assembly was gradually squeezed under pressure. Once the nominal yoke gap was achieved, the press was locked off and the assembly was allowed to cure for 12 hrs. Clamps were then inserted and the press was relaxed. Fig. 18 shows the evolution of stress in the coil during initial compression. The stress level in inner layer mid-plane region on either side is very similar indicating that the coil was loaded symmetrically. This was an issue in the mechanical model and was resolved by placing a shim between the iron mirror and aluminum bronze spacers at both ends.

The strategy was to assemble the coil with low pre-stress and if needed increase it in the subsequent thermal cycles. The mid-plane interference between the G10 shim and the iron mirror was 0.1 mm and the partial radial interference between the bronze spacer and the yoke was 0.05 mm. Once the assembly was clamped, it was transferred into the skin assembly and the bolts were tightened. End-plates were then installed. The procedure followed was very similar to that of HFDA-03A mirror magnet [TD-03-001].

Table 6 lists the stress values in the coil and in the spacer during the various stages of assembly. Note the stress level in the coil was kept below 70 MPa to avoid any possible degradation in the conductor. Note that this magnet was assembled with horizontal split yoke design compared to vertical split for the rest of magnets. Fig. 19 shows the schematic of yoked assemblies for both designs

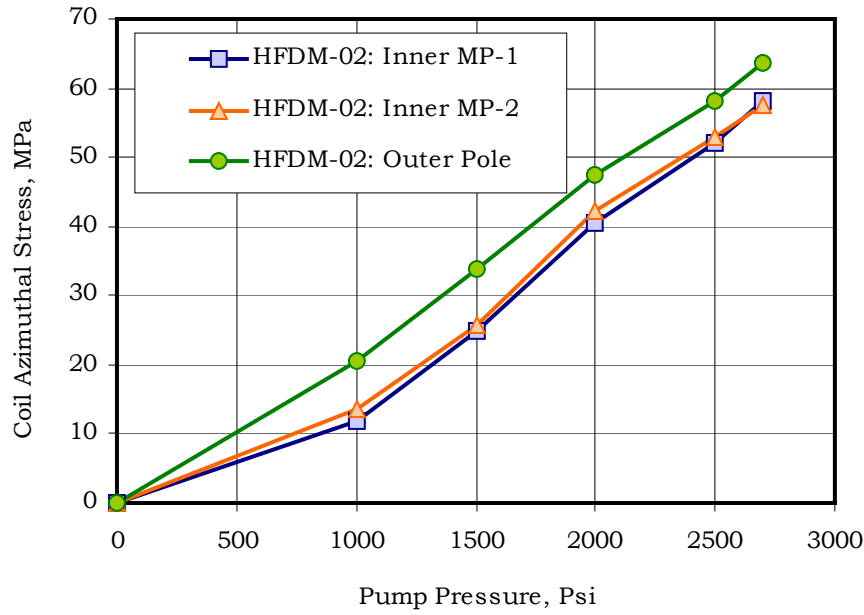


**Fig. 18:** Evolution of stress in the coil during yoking.

	YOKING/ CLAMPING	AFTER SPRING BACK	AFTER SKINNING
Coil Inner Layer Mid-Plane, MPa	41	27	35
Coil Outer Layer Pole, MPa	55	35	50
Spacer Pole in Straight Section, MPa	64	54	60
Spacer Mid-Plane in Straight Section, MPa	4	2	2

**Table 6:** Azimuthal stress in the coil and spacer during various stages of assembly.

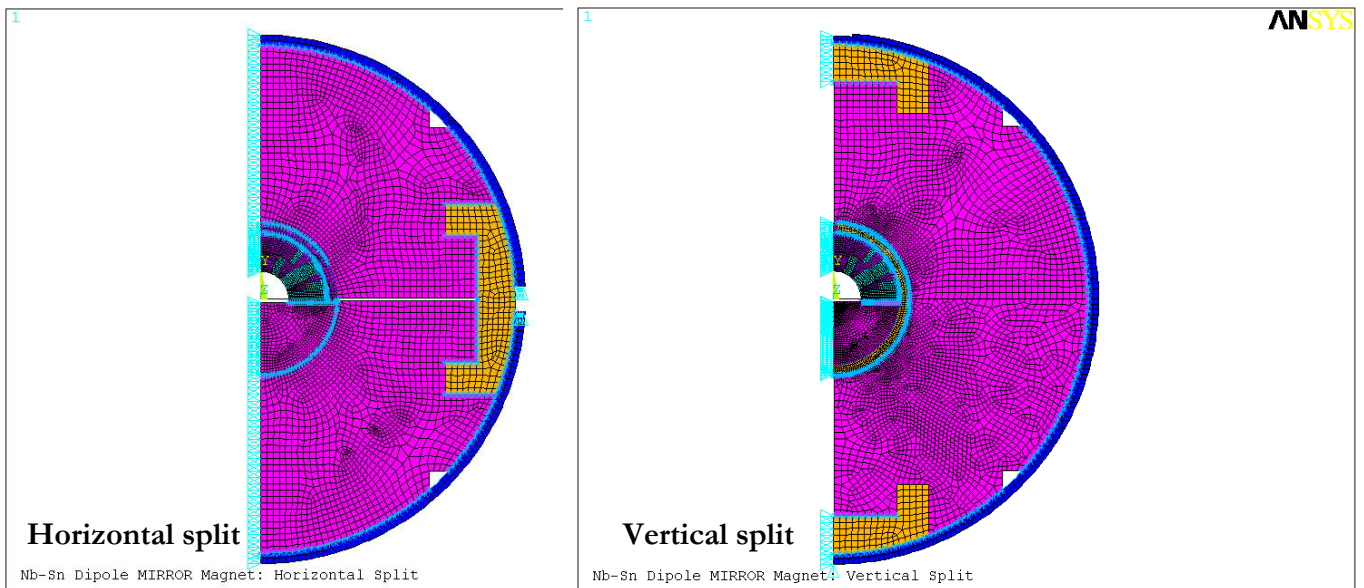


**Fig. 19:** Horizontal versus Vertical split yoke design.

## 8.0 FINAL ASSEMBLY

The lead cables were routed through the standoff plate and secured. All wires were terminated to the hypertronic connectors.

Electrical measurements were performed before shipping the magnet out to VMTF. Table 8 summarizes these measurements. Hi-pot tests were also done on the magnet and the current leakage between coil to ground, heater to ground and coil to heater was less than  $0.04\ \mu\text{A}$  at 500 V.

	RESISTANCE, $\text{m}\Omega$	INDUCTANCE, $\mu\text{H}$	Q
HFDM – 02 (R @ 0.1A, L & Q @ 1KHz)	92.95	187.251	1.79
HFDM – 02 (L & Q @ 20 Hz)		343.091	0.40

**Table 8:** *Final L-Q-R measurements on the magnet.*

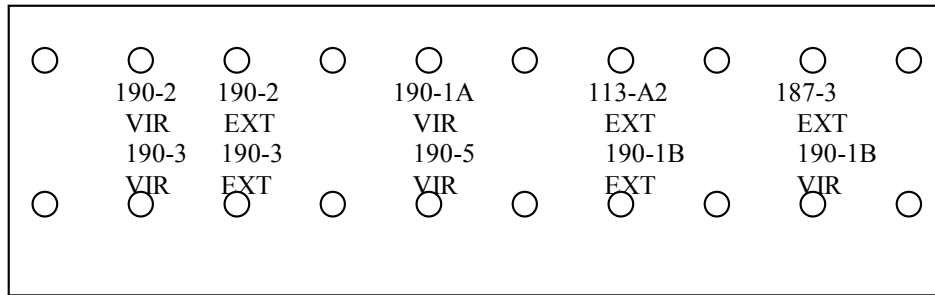
## APPENDIX

### HFDM-02 WITNESS RESULTS

#### SAMPLE LOCATIONS

LE

RE



The above is the sample location. Of these 10 samples, 9 were tested (187-3 ext. was not). Sample 113-A2 was extracted from the HFDM-01 cable just to check its performance since it belonged to an older billet.

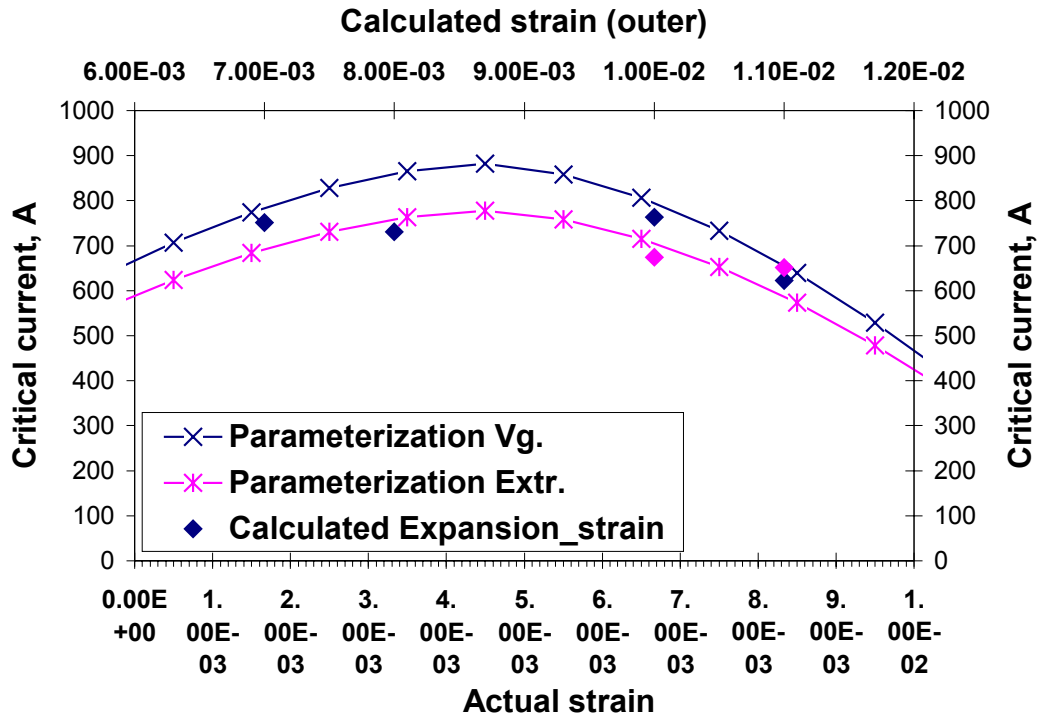
	Ic (12 T), A	n-value (12 T)	RRR
190-2 vg.	[763]	-	23
190-2 ext.	[651]	-	23
190-3 vg.	623	17	6
190-3 ext.	674	-	6
190-1B vg.	Q. 337	-	7
190-1B ext.	676	14	5
190-5 vg.	731	18	8
190-1A vg.	[751]	-	25
113-A2 ext. from HFDM01	565	15	-

The above is the table with Ic and n-value data at 12 T and RRR's. Values between “[ ]” were parameterized values from higher field data. The n-value cannot be measured when there are not enough points. One can

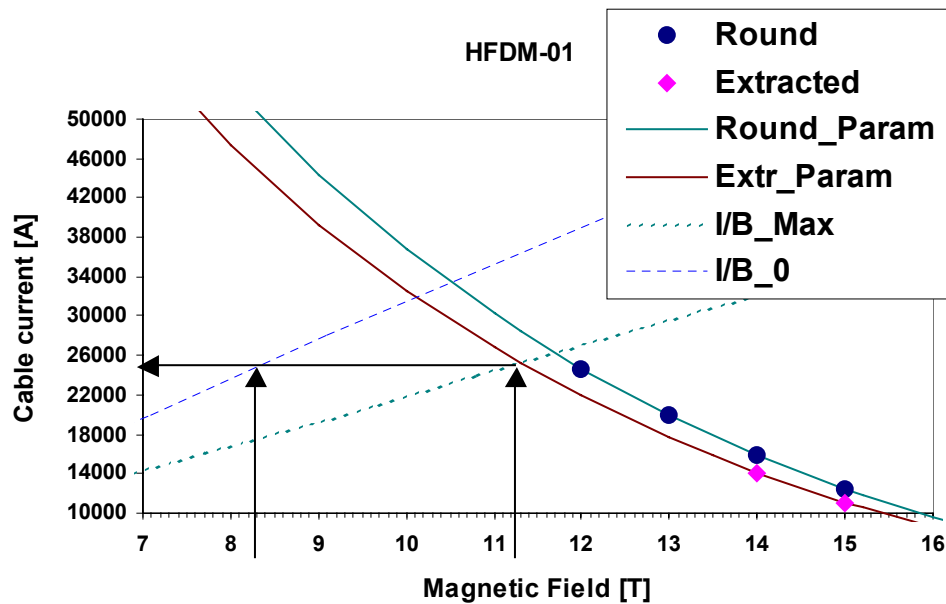
see that these Ic values have a large variation. This time barrels sizes were measured before and after reaction at both ends of each barrel.

SAMPLE #				Outer		Outer
190-3		Before HT		31.97 / 32.03		31.97 / 32.02
Virgin		After HT		32.37 / 32.46		32.25 / 32.40
190-3		Before HT		32.05		32.00 / 32.05
Extracted		After HT		32.38 / 32.46		32.25 / 32.41
190-2		Before HT		31.98 / 32.12		31.98 / 32.08
Virgin		After HT		32.33 / 32.41		32.28 / 32.41
190-A1		Before HT		31.87 / 32.03		31.88 / 31.95
Virgin		After HT		32.08 / 32.20		32.10 / 32.25
187-3		Before HT		31.97 / 32.04		31.97 / 32.03
Extracted		After HT		32.30 / 32.42		32.31 / 32.43
190-1B		Before HT		32.02 / 32.14		32.04 / 32.10
Virgin		After HT		32.23 / 32.28		32.22 / 32.30
190-5		Before HT		31.98 / 32.08		31.94 / 32.09
Virgin		After HT		32.17 / 32.37		32.26 / 32.34
190-2		Before HT		32.01 / 32.08		32.03 / 32.08
Extracted		After HT		32.31 / 32.40		32.32 / 32.55
190-1B		Before HT		31.94 / 32.11		31.92 / 32.08
Extracted		After HT		32.28 / 32.43		32.28 / 32.41
113-A2		Before HT		32.06 / 32.13		31.96 / 32.04
Extracted		After HT		32.28 / 32.34		32.20 / 32.28

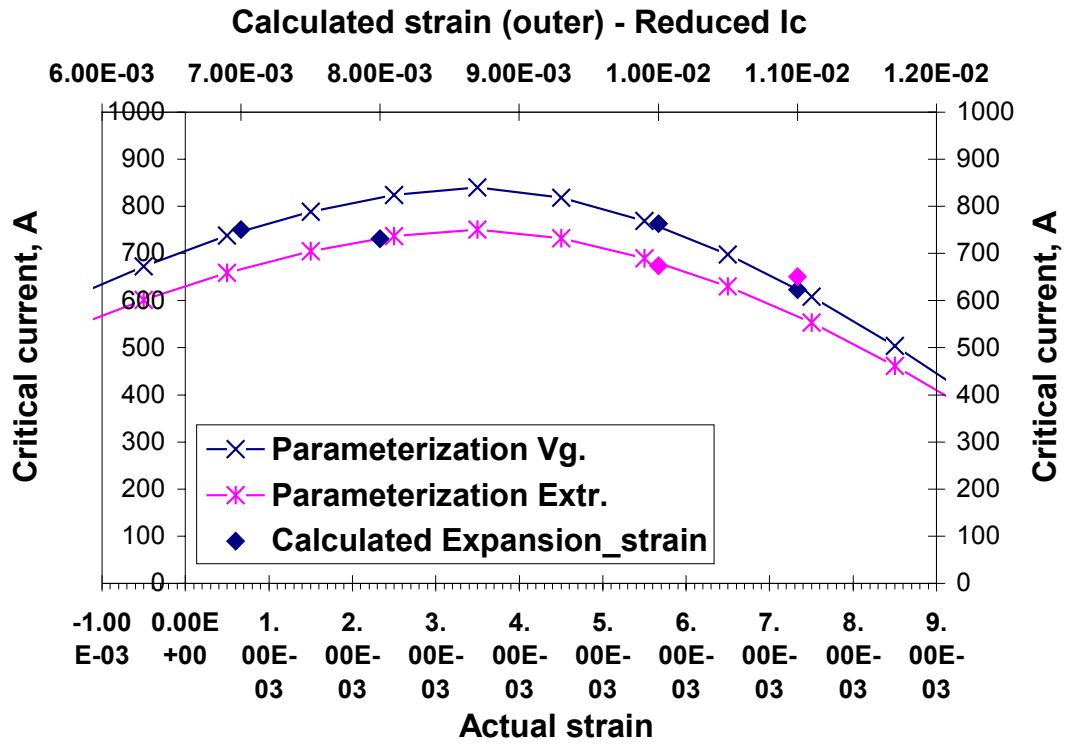
These are the results on the barrels expansion. Larger and lower values were measured because of ellipticity.



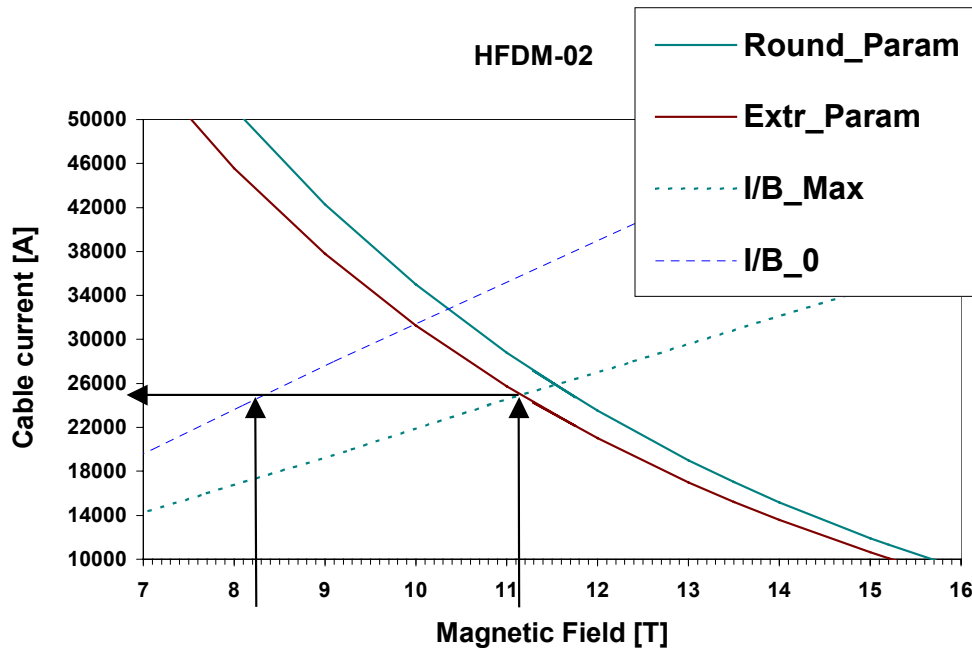
The above shows the  $I_c$  vs. the strain associated to a sample in the assumption that all of it were applied after reaction (called “calculated strain”). Blue points refer to virgin samples, pink points to extracted (note that the pink point at  $1 \cdot 10^{-2}$  of calculated strain hides another one underneath). However, since this is not true, a fit of such data points was attempted with parameterizations by varying the scale of the actual strain in the parameterized formula until a good match was obtained with the data points. *The above plot makes the further assumption that the non-strained average  $I_c$ 's of the virgin and extracted samples were the same as those found in HFDM-01 witnesses [  $I_c(12\text{ T})_{vg.} = 882\text{ A}$  and  $I_c(12\text{ T})_{ext} = 781\text{ A}$  ], where negligible expansion was measured on the barrels.*



In such a case, the short sample limits of HFDM-02 would be the same as for HFDM-01, which are shown in the above: 25230 A for a  $B_0$  of about 8.4 T and a  $B_{max}$  of about 11.3 T.



If, however, the non-strained  $I_c$  is left to vary the above fit is for instance obtained, where  $I_c(12\text{ T})_{\text{vg.}} = 840\text{ A}$  and  $I_c(12\text{ T})_{\text{ext}} = 751\text{ A}$ . The cabling degradation in such case is about 10% as in the previous case.



In this case, the short sample limits of HFDM-02 would be only slightly smaller than for HFDM-01. They are shown in the above: 24243 A for a  $B_0$  of about 8.3 T and a  $B_{\text{max}}$  of about 11.2 T.